Very high-capacity short-reach VCSEL systems exploiting multicarrier intensity modulation and direct detection

Alberto Gatto,* Debora Argenio, and Pierpaolo Boffi

Politecnico di Milano, Dipartimento di Elettronica, Informazione e Biomedica (DEIB), Policom Lab, via Ponzio 34/5, 20133, Milano, Italy

**alberto.gatto@polimi.it*

Abstract: Multicarrier intensity modulation of a bandwidth-limited long-wavelength VCSEL is exploited combined to direct detection to achieve very high capacity simple systems for short-reach applications. Tailored FDM subcarriers modulation and allocation allow to match the non-uniform frequency response of the system induced by the direct modulation and detection of the FDM signal and by the uncompensated SSMF propagation, overcoming the VCSEL bandwidth limitations. A whole transported throughput ranging from 34 Gb/s to 25 Gb/s from few hundreds meters to 20 km of SSMF propagation is experimentally demonstrated even by employing a 5-GHz band VCSEL source.

OCIS codes: (060.2330) Fiber optics communications; (140.7260) Vertical cavity surface emitting lasers.

References and links

1. M. C. Amann, E. Wong, and M. Mueller, "Energy-efficient high-speed short-cavity VCSELs," in *Proceedings of Optical Fiber Communication (OFC) Conference* (OSA, 2012), paper OTh4F.
2. W. Hofmann and D. Bimberg, "VCSEL-based light sources—scalability challenges for VCSEL-based multi-100- Gb/s systems," IEEE Photonics J. **4**(5), 1831–1843 (2012).
3. W. Hofmann, P. Moser, and D. Bimberg, "Energy-efficient VCSELs for interconnects," IEEE Photonics J. **4**(2), 652–656 (2012).
4. F. Karinou, C. Prodaniuc, N. Stojanovic, M. Ortsiefer, A. Daly, R. Hohenleitner, B. Kogel, and C. Neumeyr, "Experimental performance evaluation of equalization techniques for 56 Gb/s PAM-4 VCSEL-based optical interconnects," in *Proceedings of European Conference on Optical Communication* (OSA, 2015), paper P.4.10.
5. F. Karinou, N. Stojanovic, G. Goeger, C. Xie, M. Ortsiefer, A. Daly, R. Hohenleitner, B. Kogel, and C. Neumeyr, "28 Gb/s NRZ-OOK using 1530-nm VCSEL, direct detection and MLSE receiver for optical interconnects," in *IEEE Optical Interconnects Conference* (IEEE, 2015), pp. 20–21.
6. C. Cole, "Beyond 100G client optics," IEEE Commun. Mag. **50**(2), s58 (2012).
7. N. Yoshimoto, J. Kani, S.-Y. Kim, N. Iiyama, and J. Terada, "DSP-based optical access approaches for enhancing NG-PON2 systems," IEEE Commun. Mag. **51**(3), 58–64 (2013).
8. C. Xie, P. Dong, S. Randel, D. Pilori, P. Winzer, S. Spiga, B. Kogel, C. Neumeyr, and M. C. Amann, "Single-VCSEL 100-Gb/s short-reach system using discrete multi-tone modulation and direct detection," in *Proceedings of Optical Fiber Communication (OFC) Conference* (OSA, 2015), paper Tu2H.2.
9. G. Cossu, F. Bottoni, R. Corsini, M. Presi, and E. Ciaramella, "40 Gb/s single R-SOA transmission by optical equalization and adaptive OFDM," IEEE Photonics Technol. Lett. **25**(21), 2119–2122 (2013).
10. S. D. Le, A. Lebreton, F. Saliou, Q. Deniel, B. Charbonnier, and P. Chanclou, "Up to 60 km bidirectional transmission of a 16 Channels × 10 Gb/s FDM-WDM PON based on self-seeded reflective semiconductor optical amplifiers," in *Proceedings of Optical Fiber Communication (OFC) Conference* (OSA, 2014), paper Th3G.8.
11. A. Barbieri, G. Colavolpe, T. Foggi, E. Forestieri, and G. Prati, "OFDM versus single-carrier transmission for 100 Gbps optical communication," J. Lightwave Technol. **28**(17), 2537–2551 (2010).
12. A. Lebreton, B. Charbonnier, G. Beninca de Farias, P. Chanclou, R. Dong, J. Le Masson, and S. Menezo, "Low complexity FDM/FDMA approach for future PON", in *Proceedings of Optical Fiber Communication (OFC) Conference* (OSA, 2013), paper OTh3A.7.
13. T. Jiang and Y. Wu, "An overview: peak-to-average power ratio reduction techniques for OFDM signals," IEEE Trans. Broadcast **54**(2), 257–268 (2008).

#258759 Received 2 Feb 2016; revised 16 Mar 2016; accepted 18 Mar 2016; published 2 Jun 2016

14. H. Ochiai and H. Imai, "On the distribution of the peak-to-average power ratio in OFDM signals," IEEE Trans. Commun. **49**(2), 282–289 (2001).
15. Y. Rahmatallah and S. Mohan, "Peak-to-average power ratio reduction in OFDM systems: a survey and taxonomy," IEEE Comm. Surv. and Tutor. **15**(4), 1567–1592 (2013).
16. M. Ortsiefer, W. Hofmann, J. Rosskopf, and M.-C. Amann, "VCSELs," in *Springer Series in Optical Sciences 166* (Springer, 2013), Ch. 10.
17. M. Ortsiefer, M. Grau, J. Rosskopf, R. Shau, K. Windhorn, E. Ronneberg, G. Bohm, W. Hofmann, O. Dier, and M.-C. Amann, "InP-based VCSELs with buried tunnel junction for optical communication and sensing in the 1.3-2.3 μm wavelength range," in *20th International IEEE Semiconductor Laser Conference, Conference Digest* (2006), pp. 113–114.
18. I. Fatadin, D. Ives, and S. J. Savory, "Laser linewidth tolerance for 16-QAM coherent optical systems using QPSK partitioning," IEEE Photonics Technol. Lett. **22**(9), 631–633 (2010).
19. L. A. Neto, D. Erasme, N. Genay, P. Chanclou, Q. Deniel, F. Traore, T. Anfray, R. Hmadou, and C. Aupetit-Berthelemot, "Simple estimation of fiber dispersion and laser chirp parameters using the downhill simplex fitting algorithm," J. Lightwave Technol. **31**(2), 334–342 (2013).
20. T. L. Koch and J. E. Bowers, "Nature of wavelength chirping in directly modulated semiconductor lasers," Electron. Lett. **20**(25), 1038–1040 (1984).
21. R. C. Srinivasan and J. C. Cartledge, "On using fiber transfer functions to characterize laser chirp and fiber dispersion," IEEE Photonics Technol. Lett. **7**(11), 1327–1329 (1995).
22. ITU-T, Recommendation G.975.1 (2004)

1. Introduction

Optical communications are the most promising solution not only in long and medium-range networks, but also in short-range data network scenarios for both professional as well as consumer applications. Compared with optical transport networks, short-reach networks are much more sensitive to cost, footprint and power consumption. For this purpose, cost-effective and energy-efficient optical sources combined with direct intensity modulation (IM) and direct detection (DD) are still mandatory. In particular, short-wavelegth (in the first window of fiber communications) vertical-cavity surface-emitting lasers (VCSELs) dominate intra-datacenter communications for low-data-rate applications due to their intrinsic low cost, energy efficiency and footprint [1–3]. Nowadays, the latest advances in IM/DD long-wavelength (in the second and third fiber communications windows) VCSELs allow to achieve for example 56-Gbit/s 4-level pulse-amplitude-modulation (4-PAM) transmission on 2-km of standard single-mode fiber (SSMF) [4] and 28-Gbit/s NRZ-OOK transmission over 10 km SSMF using a high-performance Maximum Likelihood Sequence Estimator (MLSE) [5]. These results are very promising, demonstrating that the VCSEL capabilities can be exploited in combination to IM/DD approach also for short-reach networks (tens of km), for example in case of inter-datacenter links and client-optics communications [6]. However, these results are obtained using very high performance source prototypes with wide electro-optical (E/O) bandwidth (more than 15 GHz).

In order to ensure cost-effective data networks in the near future, standard devices characterized by limited E/O bandwidths should be exploited. In order to overcome the bandwidth limitation, the spectral efficiency of the transmitted signal has to be drastically increased. Fortunately, recent progress in digital signal processing (DSP) will ensure the introduction of advanced modulation formats, pulse shaping techniques and sub-carrier multiplexing even in short-reach and access scenarios [7]. Among the different methods, direct-detected orthogonal frequency division multiplexing (DD-OFDM) or discrete multi-tone (DMT) seemed interesting for overcoming E/O limitations thanks to the exploitation of hundreds of sub-carriers at very low baud rate. Recently, the employment of DD-OFDM or DMT has been proposed for enhancing the transported capacity of VCSELs in short-reach systems [8], of reflective semiconductor optical amplifier (RSOA) in addition of advanced optical filtering [9] and even in self-seeded RSOA-based wavelength division multiplexed passive optical networks (WDM-PON) [10]. Anyway, the complexity of the transmission system, the need of massive DSP and the arising of distortions due to the high peak-to-average ratio (PAPR) could limit their realistic exploitation in short-reach networks [11,12]. Its impact can be mitigated using PAPR reduction techniques, but affecting system

#258759 Received 2 Feb 2016; revised 16 Mar 2016; accepted 18 Mar 2016; published 2 Jun 2016

complexity, energy consumption and latency [13]. Since PAPR increases as the number of sub-carriers increases [14,15], a promising alternative can be frequency division multiplexing (FDM), which still permits the exploitation of multicarrier modulation but limiting the number of sub-carriers, so strongly reducing the PAPR impact and the complexity of the transmission system.

In this paper we exploit the capabilities of a multicarrier approach to suitably tailor the FDM signals in terms of modulation order and power equalization of the different sub-carriers, overcoming the bandwidth limitation of a long-wavelength 5-GHz bandwidth VCSEL and matching the not-uniform system frequency response due to IM/DD and to uncompensated SSMF propagation. In particular, thanks to an adaptive disposition of the FDM sub-carriers, a total capacity ranging from 34 Gbit/s to 25 Gbit/s from few hundreds meters to 20 km of SSMF propagation is achieved and experimented.

3. System description

In Fig. 1 the experimental setup for evaluating the performance of the proposed VCSEL-based FDM short-reach system is shown. The basic physical structure of the 1580-nm single-mode VCSEL employed in our experimentation is basically the same as described in [16,17] with optimized heat management in the cladding layers and improved bottom-mirror reflectivity. The optical single-mode spectrum shows a side mode suppression ratio beyond 40 dB over the relevant current and temperature range. The maximum emitted power is about 0.5 mW, the measured linewidth is about 8 MHz while the electro-optical bandwidth is about 5 GHz. Owing to its limited electro-optical response, the maximum transmission bit-rate achievable without strong penalties for a directly modulated OOK signal is about 8 Gb/s. In order to optimize the VCSEL modulation, taking into account its limited E/O response, the FDM signal has been suitably tailored. Specifically, the FDM signal is calculated by Matlab® and the RF signal is generated by a Tektronix 50 GS/s arbitrary-waveform-generator with 14-GHz electrical bandwidth, which drives the VCSEL current via a bias-Tee, that also combines a 9.5-mA DC current to bias the device. The VCSEL available bandwidth is divided into ten non-overlapping zero-roll-off Nyquist-shaped frequency sub-bands, carrying a different multiple-level complex modulation format. The directly modulated signal is transmitted over different lengths (100 m, 10 km and 20 km) of uncompensated SSMF. Finally, a 7.5-GHz avalanche photodiode (APD) receiver directly detects the transmitted signal, which is acquired by a Tektronix digital-storage-oscilloscope (DSO 6124C) with 8 bits vertical resolution, 40 GS/s sampling rate and 12-GHz electrical bandwidth. The off-line processing provides digital sub-carriers down-conversion, carrier phase recovery [18], symbol synchronization and demodulation. The received digital signal is then sent to a 9-taps FFE/4-taps DFE equalizer in order to compensate for the distortions due to the limited VCSEL E/O response and other band limitations of devices involved in the signal generation process.

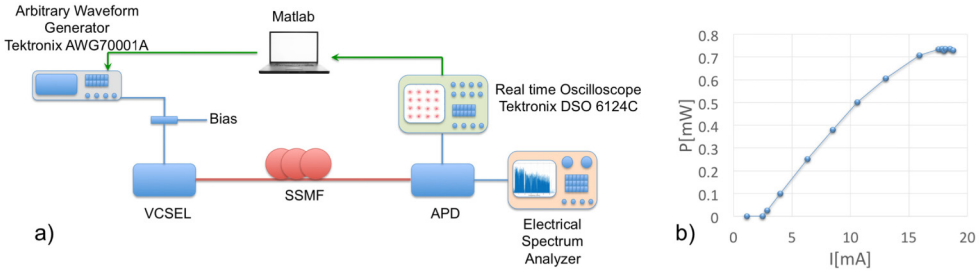

Fig. 1. (a) Experimental setup, (b) P vs I_{bias} curve for the 1580-nm VCSEL.

#258759 Received 2 Feb 2016; revised 16 Mar 2016; accepted 18 Mar 2016; published 2 Jun 2016

2. Channel description

Chromatic dispersion will lead to a different phase accumulation for each spectral component of the modulated optical signal after fiber propagation. Owing to the double-sideband spectrum achieved by VCSEL direct modulation without optical filtering at the VCSEL output, destructive beating may occur at specific frequencies after the DD process at the receiver, resulting in a frequency-selective channel that could induce significant distortions of the signal spectrum and could impose a limit on the maximum transported capacity. The frequency of the fading dips depends on the cumulated chromatic dispersion, moving towards lower frequencies for higher dispersion. Moreover, laser frequency chirp due to the direct IM has a significant impact on the frequency-fading distortion [19].

The interaction between phase and intensity modulation in a laser is described using the relation between the instantaneous frequency deviation $\Delta\upsilon(t)$ and the optical modulated power $P(t)$ [20]:

$$\Delta\upsilon(t) = \frac{\alpha}{4\pi}\left(\frac{1}{P(t)}\frac{\partial P(t)}{\partial t} + \kappa P(t)\right), \tag{1}$$

where α is the linewidth enhancement factor and κ is a laser-specific adiabatic constant related to the thermal effects, which depends on several laser parameters such as its gain saturation, carriers lifetime and confinement factor. A small-signal frequency response analysis can be exploited for modeling the VCSEL source and obtain its specific chirp coefficients [21]. For a directly modulated laser (DML), the general channel transfer function can be expressed as [19]:

$$H(\omega) = \left|\cos(\theta) - \sin(\theta)\alpha\left(1 - j\frac{\omega_c}{\omega}\right)\right| \tag{2}$$

where

$$\theta = \frac{LD\lambda_0^2\omega^2}{4\pi c}, \omega_c = \kappa P_0$$

and L is the fiber length, D the dispersion coefficient, λ_0 the wavelength of the CW source, c the speed of light and P_0 the mean optical power. Normally, the position of the frequency dips and the height of the secondary lobes are determined by an interplay of α and D, while the extent of the dips (in particular of the first one) is primarily due to ω_c.

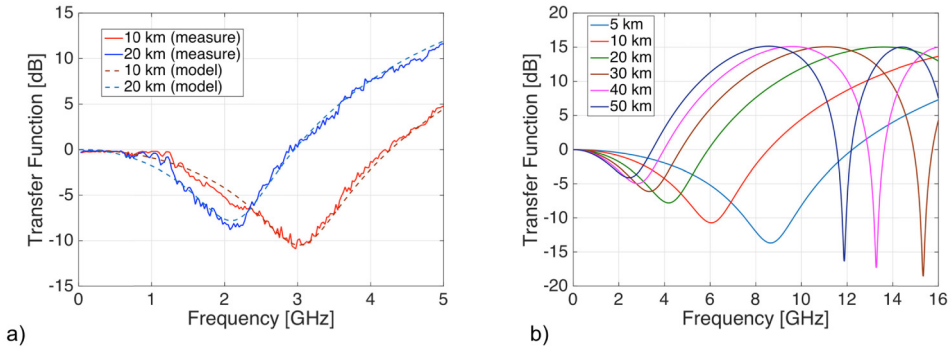

Fig. 2. (a) Measured and theoretical fiber transfer function after 10-km or 20-km SSMF propagation. (b) Theoretical frequency responses for different SSMF length.

In order to obtain the real measured fiber power transfer function to fit it by Eq. (2), the optical back-to-back contribution has to be excluded removing all the spectral distortions due to the E/O and O/E processes. In Fig. 2 the measured and theoretical frequency responses are

#258759 Received 2 Feb 2016; revised 16 Mar 2016; accepted 18 Mar 2016; published 2 Jun 2016

shown. The theoretical curves after fitting (dashed lines in Fig. 2(a)) show a good agreement with the experimental measurements, leading to $\alpha \approx 5.5$ and $\kappa \approx 10^{13}$, which are a reliable estimation of VCSEL chirp parameters. In Fig. 2(b) the theoretical transfer function calculated using the fitting parameters for different SSMF length are shown. As visible, when the cumulated dispersion increases the frequency dips move towards lower frequencies, reducing the undistorted region of the electrical spectrum. In order to limit the impact of frequency fading, the spectral dips can be filled by robust FDM sub-bands with lower spectral efficiency, like BPSK or QPSK.

3. Directly-modulated FDM VCSEL performance

In order to overcome the frequency-fading distortion and the limited E/O bandwidth of the employed VCSEL source, a tailored disposition of the sub-bands has been performed for the different SSMF lengths taken into account. In order to reduce the complexity of the transmission system, every sub-band is modulated at 1 Gbaud. No inter-subcarrier guard-band is kept, just an initial 250-MHz gap is left to ease optical carrier filtering. Hence, the FDM signal is constituted by ten subcarriers, positioning a frequency range up to 10 GHz. Since a 0-roll-off Nyquist shaping has been exploited, every sub-band fills 1 GHz of the electrical spectrum. Hence, the central frequency of the sub-bands is $n \cdot 0.75$ GHz, where n is the number of the considered sub-carrier. In Fig. 3 the results obtained in case of 10-km SSMF propagation are summarized.

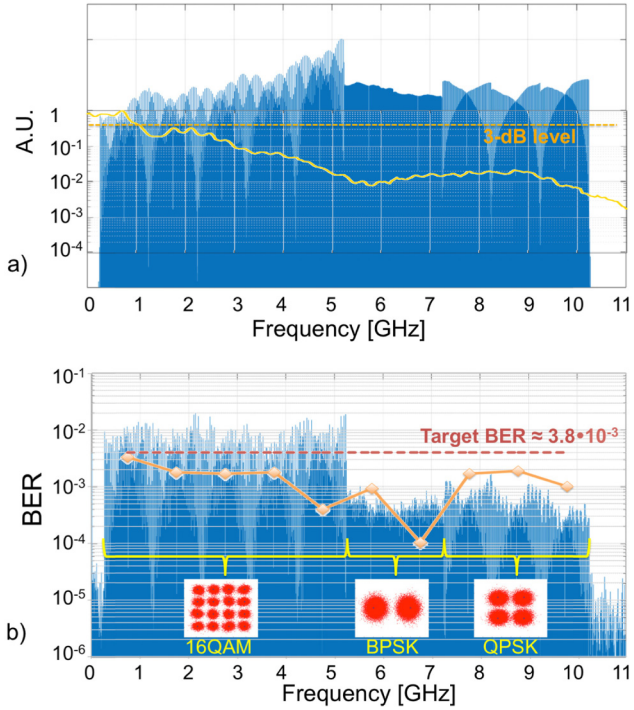

Fig. 3. (a) Generated electrical spectrum (blue) and measured power frequency response after 10-km SSMF propagation (yellow). The 3-dB level of the frequency response is identified by the orange line. (b) Received electrical spectrum (blue) and bit error rates relative to the different sub-carriers after 10-km SSMF propagation (orange).

As FDM signal generation is concerned, in order to overcome the limitations imposed by the frequency response of the whole transmission system (shown in Fig. 3(a) – yellow curve), a power equalization of the sub-bands is needed. In particular, a trade off between modulation order, subcarrier power and bit error rate associated to the single subcarrier has been

#258759 Received 2 Feb 2016; revised 16 Mar 2016; accepted 18 Mar 2016; published 2 Jun 2016

performed. At lower frequencies (for the first five central frequencies from 0.75 GHz to 4.75 GHz) higher-order modulation formats like 16-QAM have been exploited for maximizing the transported capacity, achieving 4-Gb/s data rate per subcarrier. In order to mitigate the impact of frequency fading due to chromatic dispersion, two robust BPSK sub-bands have been placed around 6 GHz. Finally, the electrical spectrum has been filled by three QPSK sub-bands at high frequencies, ranging from 7.75 GHz to 9.75 GHz, where the VCSEL bandwidth is limited, transporting an extra capacity of 2-Gbit/s per subcarrier. The equalized electrical power spectrum of the resultant 28-Gbit/s signal, generated by Matlab® and sent to the Tektronix arbitrary waveform generator, is shown in Fig. 3(a) – blue. The electrical power spectrum obtained at the receiver after 10-km SSMF propagation is shown in Fig. 3(b) – blue, while the bit error rates (BERs) are reported in orange. Thanks to the performed equalization and tailored modulation assignment, no significant difference among the sub-bands is visible. In particular, no critical penalty is noticeable around 6 GHz, i.e. where falls the frequency dip due to chromatic dispersion fading. All the ten FDM subcarriers satisfy the BER target of $3.8 \cdot 10^{-3}$ allowing the exploitation of an advanced FEC code with a 7% overhead [22].

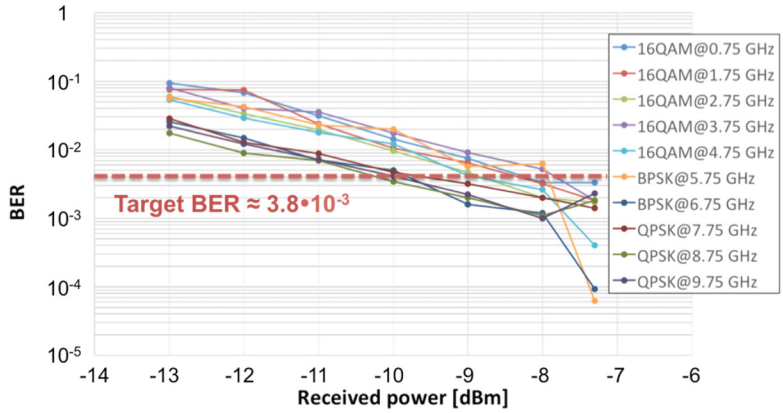

Fig. 4. BER vs received power for the different sub-carriers after 10-km SSMF propagation.

Finally, Fig. 4 presents BER curves corresponding to the different FDM sub-carriers after 10-km SSMF propagation after sub-band down-conversion, carrier phase recovery, symbol synchronization and FFE/DFE equalization. As can be seen, the target BER is reached at about −7 dBm of received power for all the sub-bands, satisfying the power budget for the10-km reach system.

The same procedure has been performed for optimizing the FDM subcarriers modulation and allocation in case of 100-m (a distance typical for intra-datacenter communications) and after 20-km SSMF propagation in presence of frequency fading occurring around 4 GHz for this last distance. The received electrical spectra and the BERs corresponding to the different ten subcarriers for the considered fiber lengths are shown in Fig. 5. Thanks to the electrical equalization of the transmitted power spectra, no significant spread among the subcarriers is visible even after 20-km SSMF propagation, leading to BER lower than the 7%-overhead FEC threshold of $3.8 \cdot 10^{-3}$. Table 1 summarizes the sub-carriers allocation (in terms of sub-carrier position in the electrical spectrum) and the total transmitted capacity in function of the propagation distance. Depending on the propagation distance, the transmitted capacity ranges from a maximum value of 34 Gb/s (for 100-m reach) to 25 Gb/s (after 20-km SSMF propagation).

#258759 Received 2 Feb 2016; revised 16 Mar 2016; accepted 18 Mar 2016; published 2 Jun 2016

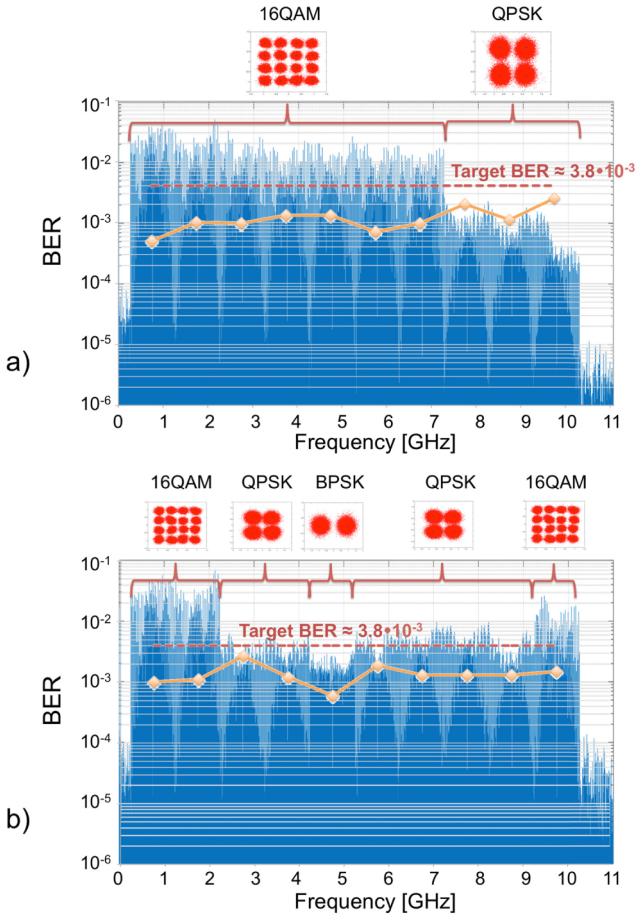

Fig. 5. Received electrical spectrum (blue) and bit error rates relative to the different sub-carriers after (a) 100-m and (b) 20-km SSMF propagation (orange).

Table 1. Allocation of the ten sub-bands (in terms of sub-carrier position) and total transported capacity for different SSMF length.

L	16QAM	QPSK	BPSK	C
100 m	1 – 7	8 – 10	–	34 Gb/s
10 km	1 – 5	8 – 10	6 – 7	28 Gb/s
20 km	1 – 2, 10	3 – 4, 6 – 9	5	25 Gb/s

4. Conclusions

Short-range transmission based on the employment of bandwidth-limited VCSEL combined with direct IM and DD is experimented by exploiting a multicarrier approach to achieve very high transported throughput. The tailored subcarrier generation in terms of modulation format and allocation allows to overcome the VCSEL band limitation and to match the non-uniform frequency response of the system. Very high capacity (34-Gb/s data rate over 100 m, 28-Gb/s over 10 km, 25-Gb/s over 20 km uncompensated SSMF reach) has been achieved even with a 5-GHz band directly modulated VCSEL in case of DD.

Acknowledgments

This work was supported by MIUR through ROAD-NGN project (PRIN2010-2011). The authors thank VERTILAS and TEKTRONIX for the support to experimentation.

#258759 Received 2 Feb 2016; revised 16 Mar 2016; accepted 18 Mar 2016; published 2 Jun 2016